Environmental Research Letters

LETTER

# Impact of fire on global land surface air temperature and energy budget for the 20th century due to changes within ecosystems

Fang Li[1,4], David M Lawrence[2] and Ben Bond-Lamberty[3]

[1] International Center for Climate and Environmental Sciences, Institute of Atmospheric Physics, Chinese Academy of Sciences, Beijing, People's Republic of China
[2] National Center for Atmospheric Research, Boulder, CO, United States of America
[3] Pacific Northwest National Laboratory, Joint Global Change Research Institute, University of Maryland, MD, United States of America
[4] Author to whom any correspondence should be addressed.

**E-mail:** lifang@mail.iap.ac.cn

**Keywords:** fire, climate, global energy budget, terrestrial ecosystems, earth system modeling, global change

Supplementary material for this article is available online

OPEN ACCESS

RECEIVED
3 December 2016

REVISED
8 March 2017

ACCEPTED FOR PUBLICATION
14 March 2017

PUBLISHED
3 April 2017



## Abstract

Fire is a global phenomenon and tightly interacts with the biosphere and climate. This study provides the first quantitative assessment and understanding of fire's influence on the global annual land surface air temperature and energy budget through its impact on terrestrial ecosystems. Fire impacts are quantified by comparing fire-on and fire-off simulations with the Community Earth System Model (CESM). Results show that, for the 20th century average, fire-induced changes in terrestrial ecosystems significantly increase global land annual mean surface air temperature by 0.18 °C, decrease surface net radiation and latent heat flux by 1.08 W $m^{-2}$ and 0.99 W $m^{-2}$, respectively, and have limited influence on sensible heat flux (−0.11 W $m^{-2}$) and ground heat flux (+0.02 W $m^{-2}$). Fire impacts are most clearly seen in the tropical savannas. Our analyses suggest that fire increases surface air temperature predominantly by reducing latent heat flux, mainly due to fire-induced damage to the vegetation canopy, and decreases net radiation primarily because fire-induced surface warming significantly increases upward surface longwave radiation. This study provides an integrated estimate of fire and induced changes in ecosystems, climate, and energy budget at a global scale, and emphasizes the importance of a consistent and integrated understanding of fire effects.

## 1. Introduction

Fire is an integral Earth system process and the primary form of terrestrial ecosystem disturbance on a global scale (Bowman *et al* 2009), burning ~400 Mha of land area each year (Randerson *et al* 2012, Giglio *et al* 2013), and damaging an average of over half of tree stems, almost all the leaves, and 10%−15% of roots when fires pass through a region (Arora and Boer 2005, van der Werf *et al* 2010). Post-fire re-growth and recovery may last for decades and even more than 100 years, so both current and historical fires exert impacts on land ecosystems (Amiro *et al* 2006, Bond-Lamberty *et al* 2007). Fire occurrence and spread are regulated by climate and weather, ecosystems, and human activities, and can feed back to them in multiple ways (Bowman *et al* 2009, Le Page *et al* 2010). Quantifying and understanding the effect of historical fire on climate and energy budget is critical in investigating fire's role in the Earth system as well as the potential broader impact of fire management, and largely determines whether and how fire should be modeled in Earth system models (ESMs) for global change research (Hantson *et al* 2016).

Fire affects the climate and energy budget in two main ways: (1) through emissions of trace gases and aerosols, and (2) through alterations to terrestrial ecosystem states and functioning (Bowman *et al* 2009). Earlier global-scale quantitative studies focused on the first way, generally finding that fire emissions

generated a negative radiative forcing and a reduction in the global surface air temperature (Ward *et al* 2012, Tosca *et al* 2013, Landry *et al* 2015, Jiang *et al* 2016). Except in our recent study of fire's influence on the global land water budget (Li and Lawrence 2017), the impact of fire through the second way or both has only been quantified at particular sites (Neary *et al* 2005, Liu *et al* 2005, Amiro *et al* 2006, Sun *et al* 2010), in a region (Bond-Lamberty *et al* 2009, Rogers *et al* 2013, Gatebe *et al* 2014), or for a specific fire (Randerson *et al* 2006).

The present study provides the first estimate and understanding of fire's impact on annual mean surface air temperature (Tas) and energy budget over global land for the 20th century through fire-induced changes within terrestrial ecosystems. Given that the interactions among climate, fire, and terrestrial ecosystems occur on a wide range of temporal and spatial scales (Bowman *et al* 2009, Randerson *et al* 2006), an Earth system model that includes global fire scheme, the Community Earth System Model version 1.2 (CESM1.2), is employed in this study. Fire impacts are quantified as the difference between CESM1.2 control (FIRE-ON) and FIRE-OFF simulations.

## 2. Simulations

### 2.1. Model platform

CESM is a global coupled model simulating the Earth's atmosphere, ocean, land, and sea ice (Hurrell *et al* 2013). The present study adopts the latest CESM-supported release version, CESM1.2 (www.cesm.ucar.edu/models/cesm1.2/), which is comprised of the Community Atmosphere Model, version 5 (CAM5, atmosphere component); Community Land Model version 4.5 with its carbon-nitrogen biogeochemical module (CLM4.5BGC, land component) (Oleson *et al* 2013, Lawrence *et al* 2011) with post-release updates to the fire module (Li and Lawrence 2017); and the Community Ice CodE, version 4 (CICE4, sea ice component).

In the real world and CESM, the land surface energy balance equation is:

$$\mathrm{SNR} = \mathrm{SH} + \mathrm{LH} + \mathrm{G}, \quad (1)$$

where surface net radiation SNR is the sum of surface net shortwave radiation absorbed by the land surface (NSW) and downward atmospheric longwave radiation (DLW) minus longwave radiation emitted from the land surface (ULW); SH is the sensible heat flux; the latent heat flux LH (i.e. $\lambda$ET, where $\lambda$ is a global constant and ET is evapotranspiration) is the sum of heat flux due to vegetation transpiration (Lt), evaporation of precipitation intercepted by the canopy (Lc), and soil evaporation(Ls); and G is the ground heat flux. A positive SH and LH transfers energy from land surface to the atmosphere, and a positive G transfers energy from land surface into the deeper soil. Based on the surface energy balance equation (equation (1)) and the Stefan-Boltzmann Law, the upward surface longwave radiation ULW can be written as:

$$\begin{aligned}\mathrm{ULW} &= \sigma T_s^4 \\ &= \mathrm{NSW} + \mathrm{DLW} - \mathrm{SH} - \mathrm{LH} - \mathrm{G}, \end{aligned} \quad (2)$$

where $\sigma$ is the Stefan-Boltzmann constant, $T_s$ is the surface temperature. Based on equation (2), we can attribute fire-induced change in surface air temperature by calculating the changes in the energy fluxes on the right hand side of the equation between FIRE-ON and FIRE-OFF simulations, as in Xu *et al* (2015) for the impact of land cover change.

The fire module in CESM1.2 (figure S1 available at stacks.iop.org/ERL/12/044014/mmedia) includes four components: agricultural fires in cropland, deforestation and degradation fires in the tropical closed forests, non-peat fires outside cropland and tropical closed forests, and peat fires (Li *et al* 2012, 2013, Li and Lawrence 2017). The burned area fraction is determined by climate and weather conditions, vegetation composition and structure, and human activities (including human deforestation rate for deforestation and degradation fires; anthropogenic ignitions and fire suppression and agricultural waste management for other non-peat fires, which are estimated by functions of population density and gross domestic product per capita). After the estimation of the burned area fraction, the fire module calculates losses and transfers of carbon and nitrogen (C/N) due to biomass and peat burning and fire-induced vegetation mortality. These changes are used to adjust C/N pools in land ecosystems. Estimates of biomass burning and plant-tissue mortality are based on PFT (plant functional type)-dependent combustion completeness factors and fire mortality factors (table S1). The fire module is the default fire model of the CESM (Oleson *et al* 2013), the Chinese Academy Sciences' Earth system model (CAS-ESM, Zeng *et al* 2014, Wang *et al* 2014), and the next version of Beijing Climate Center Climate System Model (BCC-CSM, W. P. Li personal communication 2015). It has also been partially introduced into the Dynamic Land Ecosystem Model (DLEM, Yang *et al* 2014), the GFDL's Earth System Model (LM, Rabin 2016), and the Canadian Earth System Model (CanESM, Melton and Arora 2016).

### 2.2. Experimental design

A transient run of CAM5 CLM4.5BGC-CICE4 from 1850 to 2004 is forced using time-varying 1850–2004 observed $CO_2$ concentration, land-use and land cover change (Lawrence *et al* 2012), population density data (HYDEv3.1 and CIESIN 2005, Li *et al* 2013), sea surface temperature (HadISST, Rayner *et al* 2003), and nitrogen deposition (Lamarque *et al* 2010). This transient run starts from an 1850 equilibrium (spin-up) state of CLM4.5BGC. The period 1850–1899 is taken as spin-up of the coupled atmosphere-land system. The simulation from 1900 onwards is used as

**Table 1.** Comparison between CESM1.2 simulations and benchmarks over land.

| Variable[a] | Period | Statistics[b] | CESM | Benchmarks | Sources for Benchmarks |
|---|---|---|---|---|---|
| Burned area | 1997–2004 | Avg | 452 | 357(GFED4) | GFED4 (Giglio *et al* 2013) |
| (Mha $yr^{-1}$) | | | | 511 (GFED4s) | GFED4s (Randerson *et al* 2012, van der Werf *et al* 2016) |
| Fraction (% $yr^{-1}$) | | S-Cor | 0.56[c] (GFED4), 0.62[c] (GFED4s) | | |
| Tas (no Antarctic,°C) | 1901–2004 | Avg | 12.3 | 12.6 | CRU TS3.21 (Harris *et al* 2014) |
| | | S-Cor | 0.99[c] | | |
| | | T-Cor | 0.83[c] | | |
| NSW | 2001–2004 | Avg | 129 | 0.98[c] 139 | CERES_EBAF-Surface_Ed2.8 (Kato *et al* 2013) |
| (W $m^{-2}$) | | | | | |
| DLW | | S-Cor | 310 | 312 | |
| (W $m^{-2}$) | | Avg | 0.99[c] | | |
| ULW | | S-Cor | 371 | 374 | |
| (W $m^{-2}$) | | Avg | 0.99[c] | | |
| SNR | | S-Cor | 69 | 78 | |
| ($Wm^{-2}$) | | Avg | 0.97[c] | | |
| SH(W $m^{-2}$) | 2000–2004 | S-Cor | 27 | 27∼32 | Trenberth *et al* (2009), Wild *et al* (2015) |
| LH (W $m^{-2}$) | | Avg | 39 | 38∼44 | |
| LH (no Antarctic) | 1989–2004 | Avg S-Cor | 0.93[c] | | LandFluxEval ET-all |
| | | S-Cor | | | (Mueller *et al* 2013) |

[a] 2 m surface air temperature (Tas), surface net shortwave radiation (NSW), and downward atmospheric longwave radiation (DLW), upward surface longwave radiation (ULW), surface net radiation (SNR), sensible heat flux (SH), and latent heat flux (LH) over land
[b] 20th century average (Avg), spatial correlation (S-Cor), and temporal correlation (T-Cor) between simulations and benchmarks
[c] pearson correlation passed the Student's t-test at the 0.05 significance level

the control simulation (FIRE-ON). The transient simulation is available from our earlier study (Li and Lawrence 2017). The FIRE-OFF simulation is the same as the FIRE-ON except that fire is deactivated for both spin-up and 20th century transient simulations.

All simulations are conducted using a finite volume 1.9° (latitude) × 2.5° (longitude) grid for the atmosphere and land components combined with a gx1v6 displaced pole grid for the sea ice component, and a temporal resolution of 30 minutes. The data mentioned in the last paragraph and other input data (e.g. soil color and texture, nitrogen deposition, non-$CO_2$ greenhouse gas and ozone concentration, surface emissions, present-day multi-year average lightning frequency and GDP) are provided with the CESM1.2.

In the present model setup, the pathways through which fire can affect land surface air temperature and energy budget are summarized as follows (also see figure 4, excluding the '↑' and '↓' after variables which are the results of the present study). Biomass burning transfers C/N from terrestrial ecosystems to the air and fire-induced vegetation-tissue mortality transfers C/N from live vegetation tissues to litter. Vegetation re-grows after fire. Fire-induced change in soil N availability affects the down-regulation of gross primary production (GPP, the C input flux of land ecosystems). Changes in the C cycle interact with vegetation structure (e.g. leaf area index (LAI), vegetation height). The changes in vegetation structure may lead to modifications in land states (e.g. albedo, roughness) and energy, water, and carbon fluxes, which interact with atmospheric circulation, climate, and clouds. The changes in C pools and surface climate further feed back onto the fire regime. In CESM, surface albedo affects the surface reflected shortwave radiation, and is affected by soil color, vegetation structure, snow coverage, and black carbon deposition (section 3 in Oleson *et al* 2013).

Similar to earlier studies which quantified fire's global effect (Ward *et al* 2012, Li *et al* 2014, Yue *et al* 2015, and references therein), the dynamic vegetation component in CLM4.5 B GC is inactive, and the land use and land cover change is prescribed (Lawrence *et al* 2012) and is the same for both the FIRE-ON and FIRE-OFF, so fire's impact through changing vegetation distribution is not assessed here. Moreover, the post-fire ash deposition is not modeled in CESM (the same with other ESMs), thus the impact of ash on terrestrial ecosystem N cycle is not included.

In addition, the impact of fire trace gas and aerosol emissions (also including the influence of deposition of fire black carbon emissions on surface albedo and the influence of fire-induced N deposition on terrestrial ecosystem N cycle) is not within the scope of the present study. Therefore, we use the prescribed fire trace gas and aerosol emissions for both the FIRE-ON and FIRE-OFF, rather than emissions modeled by the fire emissions module in CESM.

### 2.3. Evaluation

Overall, CESM1.2 reasonably models fire, Tas, and the energy fluxes over land (table 1). The simulated 1997–2004 global annual burned area (452 Mha $yr^{-1}$) is between values from MODIS-based global fire product GFED4 (Giglio *et al* 2013) and GFED4s (small fires included) (Randerson *et al* 2012, van der Werf

*et al* 2016) (table 1). CESM1.2 generally replicates the spatial pattern of burned area fraction (figure S2), but underestimates burned area over boreal forests in North America, shrub land in eastern Russia and Alaska, and tropical savannas in North Australia, partly due to wet biases in these regions in CESM1.2 (Li and Lawrence 2017).

The simulated average, spatial pattern, and temporal variability of land Tas during the 20th century are close to the gauge-based CRU TS3.21 (Harris *et al* 2014, table 1, figure S3). Compared with the satellite-based radiation product CERES (Kato *et al* 2013), CESM1.2 skillfully simulates the 2001–2004 downward atmospheric longwave radiation and upward surface longwave radiation (table 1, figure S4), but underestimates the surface net shrotwave radiation by 7% and net radiation by 13% mainly due to an underestimation of simulated incident shortwave radiation in the tropics (figure S4). The simulated global total of sensible and latent heat fluxes are in the range of previous estimates (Trenberth *et al* 2009, Wild *et al* 2015, table 1). The spatial pattern of simulated present-day latent heat flux is similar to LandFluxEVAL (Mueller *et al* 2013, table 1, figure S5).

## 3. Results

### 3.1. 20th century fires and induced changes within terrestrial ecosystems

The simulated global burned area averaged over the 20th century is 489 Mha $yr^{-1}$, close to the estimate of 500 Mha $yr^{-1}$ by Mouillot and Field (2005) which is based on published fire data, data on land-use practices, qualitative reports, as well as local studies that include tree ring analyses. CESM simulates a high burned area fraction in tropical savannas (location: http://questgarden.com/112/58/8/101029173956/index.htm) and southern Asia, a moderate fraction in northern Eurasia and the Rocky Mountains, and a low fraction in arid regions due to low fuel availability and in humid forests due to low fuel combustibility (figure 1(*a*)), which are generally the same as that presented in Mouillot and Field (2005).

In CESM, LAI and vegetation height are decreased in almost all post-fire regions (figures 1(*b*) and (*c*)). In total, 50% and 57% of global land area shows a statistically significant change for the two variables. Averaged over the 20th century, fire decreases global average LAI by 0.56 $m^2$ $m^{-2}$ and vegetation height by 0.87 m, significant at a 0.05 level (table 2). Fire-induced reductions in LAI and vegetation height can be supported by earlier site-level field observations across various biomes (Shackleton and Scholes 2000, Wang *et al* 2001, Furley *et al* 2008, Bond-Lamberty and Gower 2008).

Fire-induced damage in vegetation canopy significantly lowers the carbon input to the land ecosystems and allocated to vegetation tissues (figures S7(*a*) and (*b*)), and can further suppress vegetation growth and post-fire recovery of C/N pools and vegetation structure. Our estimated fire-induced changes in carbon cycle are in agreement with earlier global quantification studies (Li *et al* 2014, Yang *et al* 2015)

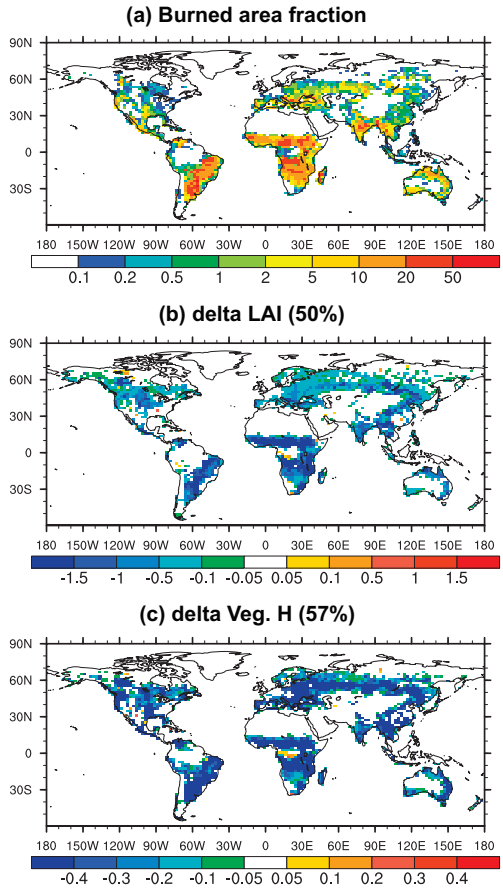


**Figure 1.** Spatial distribution of annual (*a*) burned area fraction (% $yr^{-1}$), and fire's impact (FIRE-ON minus FIRE-OFF) on annual average (*b*) leaf area index (LAI, $m^2$ $m^{-2}$) and (*c*) vegetation height (Veg. H, m) averaged over the 20th century. In (*b*) and (*c*), only regions with changes significant at the 0.05 level using the Student's t-test are shown, whose percent in global land area (%) is given in the bracket.

**Table 2.** 20th century average of annual difference (FIRE-ON minus FIRE-OFF) between FIRE-ON and FIRE-OFF simulations over global land.

| Variable[a] | Diff | Variable | Diff |
|---|---|---|---|
| Tas (°C) | +0.18[b] | NLW (W $m^{-2}$) | −1.31[b] |
| NSW (W $m^{-2}$) | +0.23 | DSW (W $m^{-2}$) | +0.39 |
| DLW (W $m^{-2}$) | +0.39 | USW (W $m^{-2}$) | +0.16[b] |
| SH (W $m^{-2}$) | −0.11 | Lt (W $m^{-2}$) | −2.69[b] |
| LH (W $m^{-2}$) | −0.99[b] | Lc (W $m^{-2}$) | −1.05[b] |
| G (W $m^{-2}$) | +0.02 | Ls (W $m^{-2}$) | +2.75[b] |
| ULW (W $m^{-2}$) | +1.70[b] | LAI ($m^2$ $m^{-2}$) | −0.56[b] |
| SNR (W $m^{-2}$) | −1.08[b] | Veg. H (m) | −0.87[b] |

[a] ground heat flux (G), downward incident shortwave radiation (DSW), upward surface reflected shortwave radiation (USW), surface net longwave radiation (NLW), LH's three components (vegetation transpiration (Lt), canopy evaporation (Lc), and soil evaporation (Ls)), leaf area index (LAI), vegetation height (Veg. H), and gross primary productivity (GPP); NSW = DSW − USW; NLW = DLW−ULW; LH = Lt + Lc + Ls; SNR = NSW + NLW

[b] difference passed the Student's t-test at the 0.05 significance level

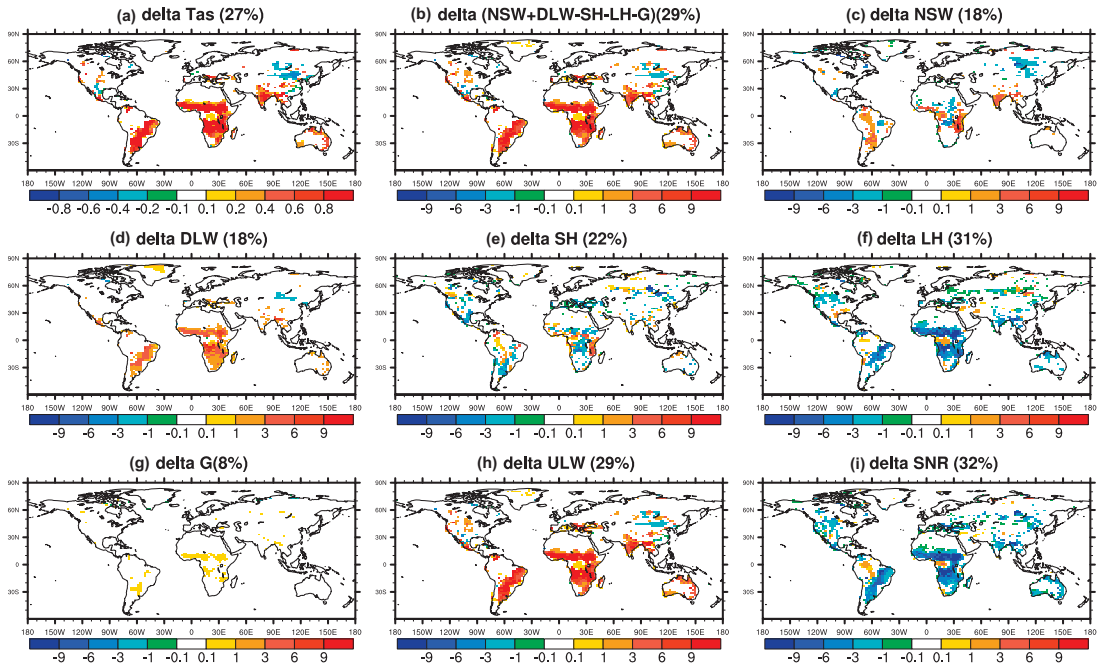


**Figure 2.** Same as figure 1, but for annual average surface air temperature (Tas, °C) and energy components (W $m^{-2}$).

and field observations (Wang *et al* 2001, Irvine *et al* 2007). Fire-induced changes in the N cycle can affect vegetation structure by changing the C cycle. Without considering fire's impact on N deposition and modeling the ash deposition (see section 2.2), even though fire-induced mortality tends to increase soil N pool, soil N availability is lower in FIRE-ON due to biomass and litter burning, lower N fixation (which is proportional to NPP in CLM4.5), and higher N leaching associated with fire-induced increases in runoff (Li and Lawrence 2017). The lower soil N availability leads to higher N limitation of photosynthesis (figure S7(*c*)) and slows the post-fire vegetation re-growth.

### 3.2. Impact on annual land surface air temperature and energy budget

The fire-induced changes within terrestrial ecosystems significantly warm the global land surface air by 0.18 °C over the 20th century (table 2). The quantified fire impact is higher than the impacts of irrigation (+0.015 °C, Sacks *et al* 2009) and land use and land cover change (–0.1 °C from Lawrence *et al* 2012, +0.008 from Findell *et al* 2007, current versus potential vegetation). With respect to the energy budget (equation (1)), fire decreases global average surface net radiation (–1.08 W $m^{-2}$), sensible heat flux (–0.11 W $m^{-2}$), and latent heat flux (–0.99 W $m^{-2}$), and little increases ground heat (table 2). Among them, fire-induced changes in surface net radiation and latent heat are significant at the level of 0.05 based on the Student's t-test, and higher than the impact of land use and land cover change (–0.19 and –0.11 W $m^{-2}$ from Lawrence *et al* 2012, and –0.14 and –0.24 W $m^{-2}$ from Findell *et al* 2007). The estimated impact of fire on these energy fluxes is sign-consistent with earlier site-level field observations (Liu *et al* 2005).

Fire impacts are most clearly seen in the tropical savannas (figure 2). Some fields are also affected significantly over regions in southern Asia, central Asia, the mid-high latitude forests in the Northern Hemisphere, and tropical closed forests. Fire generally warms the surface air, and increases the upward surface longwave radiation and downward atmospheric longwave radiation, except for regions in central Asia. Their spatial patterns are similar. Fire generally decreases latent heat (figure 2(*f*)) and surface net radiation (figure 2(*i*)), and increases ground heat (figure 2(*g*)). In total, 27%, 32%, 22%, 31%, and 8% of land areas undergo a statistically significant fire-induced change in surface air temperature, surface net radiation, sensible heat flux, latent heat flux, and ground heat flux, respectively. The result that fire reduces latent heat over most post-fire regions (figure 2(*f*)) is supported by site-based observations (Amiro *et al* 1999, Neary *et al* 2005, Sun *et al* 2010).

As shown in figure 3, fire-induced warming exhibits an upward trend for 1910–1940 and downward trend since ~1940 (figure 3(*a*)). Fire-induced reduction in latent heat is enhanced before ~1950, and waned thereafter (figure 3(*b*)). All of these trends are significant at the level of 0.05 based on the Mann–Kendall trend test. CESM simulates two periods of strong global land warming during the 20th century: 1910−1940 and since the 1970s (figure 3(*a*)), in agreement with the observations (Stocker *et al* 2013, figure S3). By changing global terrestrial ecosystems, fire intensifies the global land warming trend in the 1910−1940 period by 38% (trend: +0.019 °C $yr^{-1}$ in FIRE-ON; +0.014 °C $yr^{-1}$ in

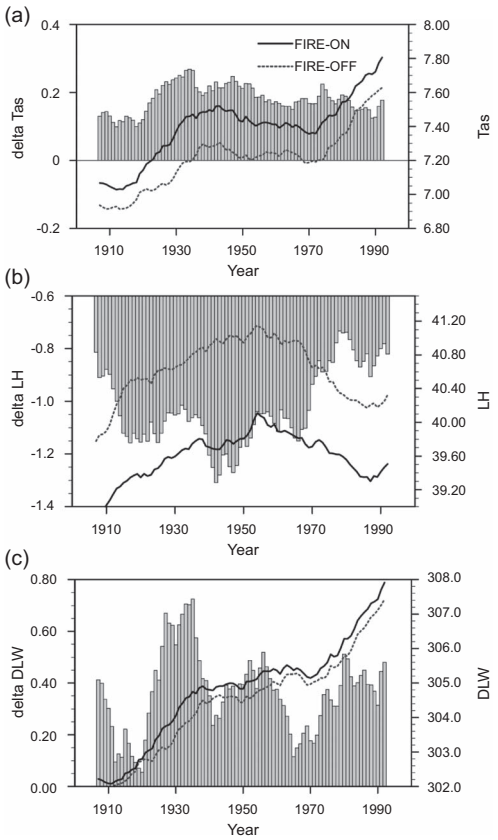


**Figure 3.** Temporal variability of FIRE-ON and FIRE-OFF simulations (lines) of (*a*) Tas (°C), (*b*) LH (W m$^{-2}$), and (*c*) DLW (W m$^{-2}$), and their difference (bars, FIRE-ON minus FIRE-OFF) over global land. A 15 year running mean is used.

FIRE-OFF) (figure 3(*a*)). Fire also weakens both the significant upward trend in global land latent heat before ~1950 and the downward trend from 1955 to ~1985 by around one third (figure 3(*b*)), and strengthens the significant upward trend in downward atmospheric longwave radiation by 26% (figure 3(*c*)) and in upward surface longwave radiation by 39% (not shown) for the period of 1910−1940. For other time periods or other energy fluxes, fire's impact on the historical trend is small or sensitive to the selected start/end points of time series, or historical trend of the target variable is insignificant. The fire-induced weaker upward trend in latent heat and stronger upward trend in atmospheric downward longwave radiation together explain the fire-induced intensification in the early 20th century global land warming trend (figure 3).

The present study also investigates the reasons for the above fire impacts. Among the surface fluxes which contribute to the change of surface air temperature (equation (2)), fire-induced change in latent heat flux is much stronger than others for the global total (table 2) and in most locations (figures 2(*b*)−(*g*)). This indicates that fire-induced change in surface air temperature is mainly caused by fire-induced reduction in latent heat. However, the cooling in central Asia mostly results from fire-induced decreases in surface net shortwave radiation and downward atmospheric longwave radiation (figure S6, figures 2(*c*) and (*d*)). The warming over some grids in equatorial African rainforests is mainly attributed to fire-induced increase in net shortwave radiation (figure 2(*c*)).

Among the energy fluxes in equation (1), fire exerts the most obvious impacts on latent heat and surface net radiation (table 2 and figures 2(*e*), (*f*), (*g*) and (*i*)). In a companion study, Li and Lawrence (2017) investigated various pathways through which fire-induced changes within land ecosystems could modify evapotranspiration (i.e. latent heat), and concluded that the reduction in latent heat could mainly be attributed to fire-induced damage in vegetation canopy (LAI). The canopy damage decreases vegetation transpiration and canopy evaporation due to lower leaf area, fewer stomata, and less canopy interception and water storage, and increases soil evaporation by exposing more of the soil to the air and sunlight (consistent with fire-induced changes in LH's three components, figures S7(*d*)−(*f*)). The less rough surface due to fire-induced reduction in vegetation height increases aerodynamic resistance and leaf boundary resistance and thus would tend to decrease latent heat flux, but at the same time lower roughness can lead to higher leaf temperature (mainly due to a reduction in sensible heat with less turbulence) and wind speed which could act to decrease stomatal resistance and increase latent heat. The net impact of fire-induced change in vegetation height is small.

Fire-induced change in surface net radiation primarily responds to fire-induced change in upward surface longwave radiation (table 2, figures 2(*c*), (*d*), (*h*) and (*i*)). There is a positive feedback loop among changes in surface temperature, upward surface longwave radiation, and downward atmospheric longwave radiation due to fire. That is, fire-induced surface warming (figure S7(*h*)) enhances upward surface longwave radiation (figure 2(*h*)) and then downward atmospheric longwave radiation (figure 2 (*d*)), which further provides more energy to warm land surface.

In addition, fire-induced change in annual surface net shortwave radiation (figure 2(*c*)) is mainly caused by fire-induced change in incident shortwave radiation (figure S7(*i*)) that responds to the fire-induced change in the coverage of low-level and mid-level clouds (figure S7(*j*)). Lower cloud coverage reflects less solar radiation and thus intensifies the incident solar radiation, and vice versa. The change in surface albedo due to fire can also affect the surface net shortwave radiation. Fire increases the surface albedo, except for regions in tropical savannas and southern Asia due to the dark soil color (Lawrence and Chase 2007) (figure S7(*k*)). The reduced surface net shortwave radiation in central Asia (figure 2(*c*)) is co-caused by fire-induced higher surface albedo and higher coverage of low-level and mid-level clouds (figures S7(*j*) and (*k*)).

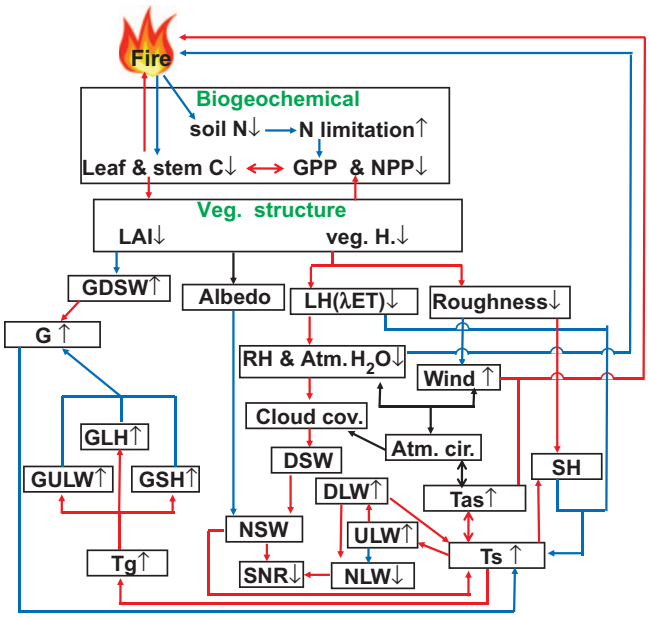


**Figure 4.** Schematic of fire's influence on land surface air temperature and energy budget for most regions. '↑' ('↓') after a variable indicates increase (decrease) in the variable due to fire; red (blue) arrow connecting two variables indicates a positive (negative) response; black arrow connecting two variables (without '↑'and '↓' after a variable) means that the sign of response (the sign of fire-induced change in the variable) is varied with region and environmental conditions; RH is relative humidity; Tg, GDSW, GLH, GULW and GSH are ground temperature, ground downward incident shortwave radiation, ground latent heat flux, ground upward longwave radiation, and ground sensible heat, respectively.

## 4. Discussion

Using CESM1.2, we investigated the mechanisms related to fire's impact on global land surface air temperature and energy budget. As summarized in figure 4, from a global perspective, leaf and stem carbon pools are decreased due to biomass burning and fire-induced vegetation mortality, which leads to a significant reduction in vegetation canopy (LAI) and vegetation height. Fire-induced changes in vegetation structure decrease carbon input of land ecosystems that, in turn, suppresses recovery of vegetation structure in post-fire regions. Fire generally decreases latent heat flux mainly due to fire-induced damage in vegetation canopy, which is the primary reason for fire-induced increase in surface air temperature. Surface warming increases upward surface longwave radiation and further reduces the surface net radiation. Global fire impacts could be enhanced by three positive feedback loops: (1) fire-induced changes in vegetation structure and carbon cycle within terrestrial ecosystems, (2) fire-induced changes in surface temperature, upward surface longwave radiation, and downward atmospheric longwave radiation, and (3) fire and fire-induced hotter and drier surface air and higher wind speed. With respect to (3), lower surface air relative humidity and higher wind speed due to fire were identified in our companion paper (Li and Lawrence 2017).

Prior studies evaluated the impact of fire emissions, the other main pathway through which fire can affect climate and energy budget. Fire impacts through emitting trace gases and aerosols and through perturbing the terrestrial ecosystem states are very different. From a global perspective, the former leads to cooling over land, mainly by reducing net shortwave radiation (Ward *et al* 2012, Tosca *et al* 2013, Jiang *et al* 2016), while the latter leads to warming, mainly by significantly reducing latent heat flux (explored in this study). Many earlier studies have highlighted the global and regional impact of the latter on regional and global carbon cycle (Bond-Lamberty *et al* 2007, Li *et al* 2014, Yang *et al* 2015, and references therein). This study shows that, even in a non-carbon view, the latter should be considered when one estimates the global fire impact, and its modeling should be included in Earth system models.

Two main sources of uncertainty in our estimates are worth noting. First, model biases in CESM will affect our estimates of fire impacts. For example, the wet bias in North American boreal forests leads to a big underestimation of burned area and therefore fire impacts. Second, the vegetation distribution in our CESM simulations is prescribed, although other ecosystem characteristics (e.g. LAI, biomass, vegetation height, and carbon fluxes) are dynamically simulated. Therefore, the effect of fire on climate and surface energy budget through changing vegetation distribution is not accounted for in our present estimates, as did most prior global quantitative studies of fire impact. Prior studies (San José *et al* 1998, Murphy and Bowman 2012) reported that fire could limit tree cover in tropical savannas. Not considering fire's impact on vegetation distribution likely results in an underestimation of fire-induced warming and decrease in latent heat in this region given that higher

tree coverage in the tropics in FIRE-OFF tends to cool the land and increase latent heat based on earlier studies of vegetation-climate interaction (Bonan 2008, Levis 2010). On the other hand, in the North American boreal forests, Rogers and Randerson (2011) reported that ignoring competition between different vegetation types would lead to faster vegetation re-growth and underestimate the increase in albedo due to non-peat fires (so fire-induced surface cooling).

The two factors (the wet bias in CESM and ignoring the impact of fire-induced changes in vegetation distribution) may explain why the present study does not reproduce the fire-induced significant cooling in the North American boreal forests shown in the regional study of Rogers *et al* (2013). Rogers *et al* (2013) used the observed present-day burned area, and the estimated fire-induced change in vegetation distribution that was derived by attributing all changes in land cover to fire. For a global study, a Dynamic Global Vegetation Models (DGVM) is the most suitable tool for investigations into it because climate, $CO_2$, and land use may also result in land cover change. However, existing DGVMs exhibited a big difference in their estimates of fire effects on regional and global vegetation distribution (Bond *et al* 2005, Scheiter and Higgins 2009, Poulter *et al* 2015). More observations and understanding of the related processes are required to lower the uncertainties before DGVMs can be reliably used to quantify fire impact on climate.

Earlier researches presented an obvious albedo change over burnt sites in the North American boreal forest (Randerson *et al* 2006, Amiro *et al* 2006), which is not reproduced in the present study. In addition to the large underestimation of burned area in this region in CESM and lack of representing fire's impacts on vegetation distribution (see Para. 3 in this section), this discrepancy may also result from the different spatial scales of CESM and field experiments. In CESM, fire's impacts on ecosystems occur on PFT or column (all vegetation PFTs share a column) level, while in the real world they are often over some sub-grid patches. If the total area of the burnt patches is small, when the PFT/column-average are calculated as in CESM, fire's impacts on ecosystems and induced changes in energy fluxes and climate will be weakened and may become statistically insignificant, and even have the opposite-sign if fire's indirect impacts outside the patches are sign-opposite and strong. This is an ongoing problem for comparison of ESM results with field studies (e.g. Shao *et al* 2013).

## Acknowledgments

This study is co-supported by the National Natural Science Foundation of China (41475099), the State Key Project for Basic Research Program of China (2010CB951801), and the China Scholarship Council. DML is supported by the U.S. Department of Energy (DE-FC03-97ER62402/A0101). BBL was supported as part of the Accelerated Climate Modeling for Energy (ACME) project, funded by the U.S. Department of Energy, Office of Science, Office of Biological and Environmental Research. We are grateful to Z-D Lin and F Zhang from the Institute of Atmospheric Physics, Chinese Academy of Sciences, R E Dickinson from the University of Texas at Austin, and E. Kluzek, S Levis (Now in the Climate Corporation), and P Lawrence from NCAR, and Y-Q Jiang from the Nanjing University for helpful discussions. We also thank two anonymous reviewers for their valuable comments and suggestions, editors for handling this paper, and GFED group for making GFED4 and GFED4s global fire products available. Computing resources were provided by the NCAR, which is sponsored by the National Science Foundation.

## References

Amiro B D, MacPherson J I and Desjardins R L 1999 BOREAS flight measurements of forest-fire effects on carbon dioxide and energy fluxes *Agric. For. Meteorol.* **96** 199–208

Amiro B D *et al* 2006 The effect of post-fire stand age on the boreal forest energy balance *Agr. Forest Meteorol.* **140** 41–50

Arora V K and Boer G J 2005 Fire as an interactive component of dynamic vegetation models *J. Geophys. Res.* **110** G02008

Bonan G B 2008 *Ecological Climatology: Concepts and Applications* 2nd edn (Cambridge: Cambridge University Press) p 550

Bond W J, Woodward F and Midgley G F 2005 The global distribution of ecosystems in a world without fire *New Phytol.* **165** 525–38

Bond-Lamberty B, Peckham S D, Ahl D E and Gower S T 2007 The dominance of fire in determining carbon balance of the central Canadian boreal forest *Nature* **450** 89–92

Bond-Lamberty B, Peckham S D, Gower S T and Ewers B E 2009 Effects of fire on regional evapotranspiration in the central Canadian boreal forest *Glob. Change Biol.* **15** 1242–54

Bond-Lamberty B and Gower S T 2008 Decomposition and fragmentation of coarse woody debris: re-visiting a boreal black spruce chronosequence *Ecosystems* **11** 831–40

Bowman D M J S *et al* 2009 Fire in the earth system *Science* **324** 480–4

CIESIN 2005 *Gridded population of the world version 3(GPWv3): Population density grids* NASA Socioeconomic Data and Applications Center (SEDAC), New York (http://sedac.ciesin.columbia.edu/data/set/gpw-v3-population-density)

Findell K L, Shevliakova E, Milly P C D and Stouffer R J 2007 Modeled impact of anthropogenic land cover change on climate *J. Clim.* **20** 3621–34

Furley P A, Rees R M, Ryan C M and Saiz G 2008 Savanna burning and the assessment of long-term fire experiments with particular reference to Zimbabwe *Prog. Phys. Geogr.* **32** 611–34

Gatebe C K, Ichoku C M, Poudyal R, Roman M O and Wilcox E 2014 Surface albedo darkening from wildfires in northern sub-Saharan Africa *Environ. Res. Lett.* **9** 065003

Giglio L, Randerson J T and van der Werf G R 2013 Analysis of daily, monthly, and annual burned area using the fourth-generation Global Fire Emissions Database (GFED4) *J. Geophys. Res. Biogeosci.* **118** 317–28

Hantson S *et al* 2016 The status and challenge of global fire modeling *Biogeosciences* **13** 3359–75

Harris I, Jones P D, Osborn T J and Lister D H 2014 Updated high-resolution grids of monthly climatic observations—the CRU TS310 dataset *Int. J. Climatol.* **34** 623–42

Hurrell J W *et al* 2013 The Community Earth System Model: a framework for collaborative research *Bull. Am. Meteorol. Soc.* **94** 1339–60

Irvine J, Law B E and Hibbard K A 2007 Postfire carbon pools and fluxes in semiarid ponderosa pine in central oregon *Glob. Change Biol.* **13** 1748–60

Jiang Y, Lu Z, Liu X, Qian Y, Zhang K, Wang Y and Yang X 2016 Impacts of global wildfire aerosols on direct radiative, cloud and surface-albedo forcings simulated with CAM5 *Atmos. Chem. Phys.* **16** 14805–24

Kato S *et al* 2013 Surface irradiances consistent with CERES-derived top-of-atmosphere shortwave and longwave irradiances *J. Clim.* **26** 2719–40

Lamarque J F *et al* 2010 Historical 1850–2000 gridded anthropogenic and biomass burning emissions of reactive gases and aerosols: methodology and application *Atmos. Chem. Phys.* **10** 7017–39

Landry J S, Matthews H D and Ramankutty N 2015 A global assessment of the carbon cycle and temperature responses to major changes in future fire regime *Clim. Change* **133** 179–92

Lawrence D M *et al* 2011 Parameterization improvements and functional and structural advances in version 4 of the community land model *J. Adv. Model. Earth Syst.* **3** M03001

Lawrence P J and Chase T N 2007 Representing a MODIS consistent land surface in the community land model (CLM 3.0) *J. Geophys. Res* **112** G01023

Lawrence P J *et al* 2012 Simulating the biogeochemical and biogeophysical impacts of transient land cover change and wood harvest inthe community climate system model (CCSM4) from 1850 to 2100 *J. Clim.* **25** 3071–95

Le Page Y, Oom D, Silva J, Jönsson P and Pereira J 2010 Seasonality of vegetation fires as modified by human action: observing the deviation from eco-climate fire regimes *Glob. Ecol. Biogeogr.* **19** 575–88

Levis S 2010 Modeling vegetation and land use in models of the earth system *WIREs Clim. Change* **1** 840–56

Li F, Zeng X and Levis S 2012 A process-based fire parameterization of intermediate complexity in a dynamic global vegetation mode *Biogeosciences* **9** 2761–80

Li F, Levis S and Ward D S 2013 Quantifying the role of fire in the earth system—Part 1: improved global fire modeling in the community earth system model CESM1 *Biogeosciences* **10** 2293–314

Li F, Bond-Lamberty B and Levis S 2014 Quantifying the role of fire in the earth system—Part 2: impact on the net carbon balance of global terrestrial ecosystems for the 20th century *Biogeosciences* **11** 1345–60

Li F and Lawrence D M 2017 Role of fire in the global land water budget during the 20th century through changing ecosystems *J. Clim.* **30** 1893–908

Liu H P, Randerson J T, Lindfors J and Chapin F S III 2005 Changes in the surface energy budget after fire in boreal ecosystems of interior Alaska: an annual perspective *J. Geophys. Res.* **110** D13101

Melton J R and Arora V K 2016 Competition between plant functional types in the canadian terrestrial ecosystem model (CTEM) v. 2.0 *Geosci. Model Dev.* **9** 323–61

Mouillot F and Field C B 2005 Fire history and the global carbon budget: A 1° × 1° fire history reconstruction for the 20th century *Glob. Change Biol.* **11** 398–420

Mueller B *et al* 2013 Benchmark products for land evapotranspiration: LandFlux-EVAL multi-data set synthesis *Hydrol. Earth Syst. Sci.* **17** 3707–20

Murphy B P and Bowman D M J S 2012 What controls the distribution of tropical forest and savanna? *Ecol. Lett.* **15** 748–58

Neary D G, Ryan K C and DeBano L F 2005 *Wildland Fire in Ecosystems: Effects of Fire on Soils and Water Gen. Tech. Rep. RMRS-GTR-42-vol.4* (Ogden UT: U.S. Department of Agriculture Forest 724 Service Rocky Mountain Research Station) p 250

Oleson K W *et al* 2013 Technical description of version 4.5 of the Community Land Model (CLM) *NCAR Tech. Note* NCAR/TN-503+STR p 434

Poulter B *et al* 2015 Sensitivity of global terrestrial carbon cycle dynamics to variability in satellite-observed burned area *Glob. Biogeochem. Cycles* **29** 207–22

Rabin S S 2016 *Investigating the impact of agricultural fire management practices on the terrestrial carbon cycle PhD thesis* (Princeton University) p 133 (http://arks.princeton.edu/ark:/88435/dsp01k3569674p)

Randerson J T *et al* 2006 The impact of boreal forest fire on climate warming *Science* **314** 1130–2

Randerson J T, Chen Y, van der Werf G R, Rogers B M and Morton D C 2012 Global burned area and biomass burning emissions from small fires *J. Geophys. Res.* **117** G04012

Rayner N A *et al* 2003 Global analyses of sea surface temperature, sea ice, and night marine air temperature since the late nineteenth century *J. Geophys. Res.* **108** 4407

Rogers B M and Randerson J T 2011 *Consequences of post-fire succession for carbon and energy fluxes in CLM* Joint Land and Biogeochemistry group meeting (Boulder) (www.cesm.ucar.edu/working_groups/Land/Presentations/Joint_Land_BGC_Chemistry11/rogers_landbgc11.pdf)

Rogers B M, Randerson J T and Bonan G B 2013 High-latitude cooling associated with landscape changes from North American boreal forest fires *Biogeosciences* **10** 699–718

Sacks W J, Cook B I, Buenning N, Levis S and Helkowski J H 2009 Effects of global irrigation on the near-surface climate *Clim. Dyn.* **33** 159–75

San José J J, Montes R A and Farinas M R 1998 Carbon stocks and fluxes in a temporal scaling from a savanna to a semi-deciduous forest *Forest Ecol. Manag.* **105** 251–62

Scheiter S and Higgins S I 2009 Impacts of climate change on the vegetation Africa: an adaptive dynamic vegetation modeling approach *Glob. Change Biol.* **15** 2224–46

Shackleton C M and Scholes R J 2000 Impact of fire frequency on woody community structure and soil nutrients in the Kruger National Park *Koedoe* **43** 75–81

Shao P, Zeng X, Sakaguchi K, Monson R K and Zeng X 2013 Terrestrial carbon cycle: climate relations in eight CMIP5 earth system models *J. Clim.* **26** 8744–64

Stocker T F *et al* 2013 *Climate Change 2013: The physical Science Basis Contribution of Working Group I to the Fifth Assessment Report of the Intergovernmental Panel on Climate Change* (Cambridge: Cambridge University Press) p 1535

Sun G *et al* 2010 Energy and water balance of two contrasting loblolly pine plantations on the lower coastal plain of North Carolina USA *For. Ecol. Manage.* **259** 1299–310

Tosca M G, Randerson J T and Zender C S 2013 Global impact of smoke aerosols from landscape fires on climate and the Hadley circulation *Atmos. Chem. Phys.* **13** 5227–41

Trenberth K E, Fasullo J T and Kiehl J 2009 Earth's global energy budget *Bull. Am. Meteorol. Soc.* **90** 311–23

van der Werf G R *et al* 2010 Global fire emissions and the contribution of deforestation, savanna, forest, agricultural, and peat fires 1997–2009 *Atmos. Chem. Phys.* **10** 11707–35

van der Werf G R *et al* 2016 GFED4 with small fires (GFED4.1s) *Global Fire Emissions Database* (www.falw.vu/~gwerf/GFED/GFED4/) (Accessed: 27 May 2016)

Wang C K, Gower S T, Wang Y H, Zhao H X, Yan P and Bond-Lamberty B 2001 The influence of fire on carbon distribution and net primary production of boreal Larixgmelinii forests in north-eastern China *Glob. Change Biol.* **7** 719–30

Wang H J, Zhu J and Pu Y F 2014 Progress and challenge of earth system modeling *Sci. China Phys. Mech. Astron.* **10** 1116–26 (in Chinese)

Ward D S, Kloster S, Mahowald N M, Rogers B M, Randerson J T and Hess P G 2012 The changing radiative forcing of fires: global model estimates for past, present and future *Atmos. Chem. Phys.* **12** 10857–86

Wild M et al 2015 The energy balance over land and oceans: an assessment based on direct observations and CMIP5 climate models *Clim. Dyn.* **44** 1–37

Xu Z, Mahmood R, Yang Z, Fu C and Su H 2015 Investigating diurnal and seasonal climatic response to land use and land cover change over monsoon Asia with the Community Earth System Model *J. Geophys. Res. Atmos.* **120** 1137–52

Yang J, Tian H, Tao B, Ren W, Kush J, Liu Y and Wang Y 2014 Spatial and temporal patterns of global burned area in response to anthropogenic and environmental factors: reconstructing global fire history for the 20th and early 21st centuries *J. Geophys. Res. Biogeosci.* **119** 249–63

Yang J, Tian H, Tao B, Ren W, Lu C, Pan S, Wang Y and Liu Y 2015 Century-scale patterns and trends of global pyrogenic carbon emissions and fire influences on terrestrial carbon balance *Glob. Biogeochem. Cycles* **29** 1549–66

Yue C, Ciais P, Cadule P, Thonicke K and van Leeuwen T T 2015 Modelling the role of fires in the terrestrial carbon balance by incorporating SPITFIRE into the global vegetation model ORCHIDEE—Part 2: carbon emissions and the role of fires in the global carbon balance *Geosci. Model Dev.* **8** 1321–38

Zeng X, Li F and Song X 2014 Development of the IAP dynamic global vegetation model *Adv. Atmos. Sci.* **31** 505–14